CHAPTER EIGHT

An Invariant Approach to the Study of Fluctuating Asymmetry: Developmental Instability in a Mouse Model for Down Syndrome

Joan T. Richtsmeier, Theodore M. Cole III, and Subhash R. Lele

INTRODUCTION

Aneuploidy refers to the condition where the number of chromosomes within an organism is not an exact multiple of the haploid number. Examples of aneuploidy include monosomy (a single chromosome instead of a pair exists for a given chromosome) and trisomy (three copies of a chromosome are present for a given chromosome). Trisomy 21 (Ts21) or Down syndrome (DS) is the

Joan T. Richtsmeier • Department of Anthropology, The Pennsylvania State University, University Park, PA 16802 and Center for Craniofacial Development and Disorders, The Johns Hopkins University, Baltimore, MD 21205. **Theodore M. Cole III** • Department of Basic Medical Science, School of Medicine, University of Missouri—Kansas City, Kansas City, MO 64108.
Subhash R. Lele • Department of Mathematical and Statistical Sciences, University of Alberta, Edmonton, Alberta, Canada T6G 2G1.

Modern Morphometrics in Physical Anthropology, edited by Dennis E. Slice.
Kluwer Academic/Plenum Publishers, New York, 2005.

most frequent live-born aneuploidy in humans, occurring in approximately one in 700 live births. The cause of Ts21 is most commonly nondisjunction during meiosis (Antonarakis, 1991; Antonarakis et al., 1992, 1993), but little is known about the mechanisms responsible for developmental anomalies associated with the DS phenotype.

Two ideas have been articulated about the cause of anomalies associated with Ts21. The first is that specific genes on Chr 21, when occurring in triplicate, cause the production of particular phenotypes (Delabar, 1993; Korenberg, 1991; Korenberg et al., 1990, 1994). The second is that Ts21 phenotypes result from a generalized genetic imbalance that causes amplified *developmental instability* (DI) produced by altered responses to genetic and environmental factors to which all individuals are exposed. This idea was proposed by Hall (1965) and supported by Shapiro and others (Greber-Platzer et al., 1999; Shapiro, 1975, 1983, 2001), who suggested that the observation of increased variability in linear measurements of many features in DS, as compared to unaffected individuals, supported this idea. The developmental mechanisms that underlie DI remain largely unexplained, however (Hallgrímsson and Hall, 2002).

Bilateral symmetry is a phylogenetically widespread characteristic of many complex organisms (Palmer, 1996). In those organisms that tend toward bilateral symmetry, there is a midline plane that divides the body into right and left halves (Figure 1). Midline symmetry is secured by ontogenetic and phylogenetic mechanisms, so that the breaking of symmetry is a relatively rare event and, therefore, of interest to biologists. Fluctuating asymmetry (FA), the variance of deviations from perfect symmetry, has been proposed and is widely used as a measure of DI (Palmer and Strobeck, 1992; Polak, 2003). Since a single genome controls the development of both the left and right sides, and the environment is typically the same for both sides, the expectation is that the two sides of an organism are replicates, or mirror images of each other. Deviations from symmetry are thought to represent the effects of random perturbations during development.

It is commonly held that the development of the organism is driven by a plan that includes perfect symmetry for traits that occur bilaterally. Even in a stable environment, however, small random perturbations of biological processes produce phenotypic deviations from the ideal. These perturbations, commonly called *developmental noise*, result in part from the accumulation of the products of stochastic gene expression mechanisms (see Kirschner and Gerhart, 1998;

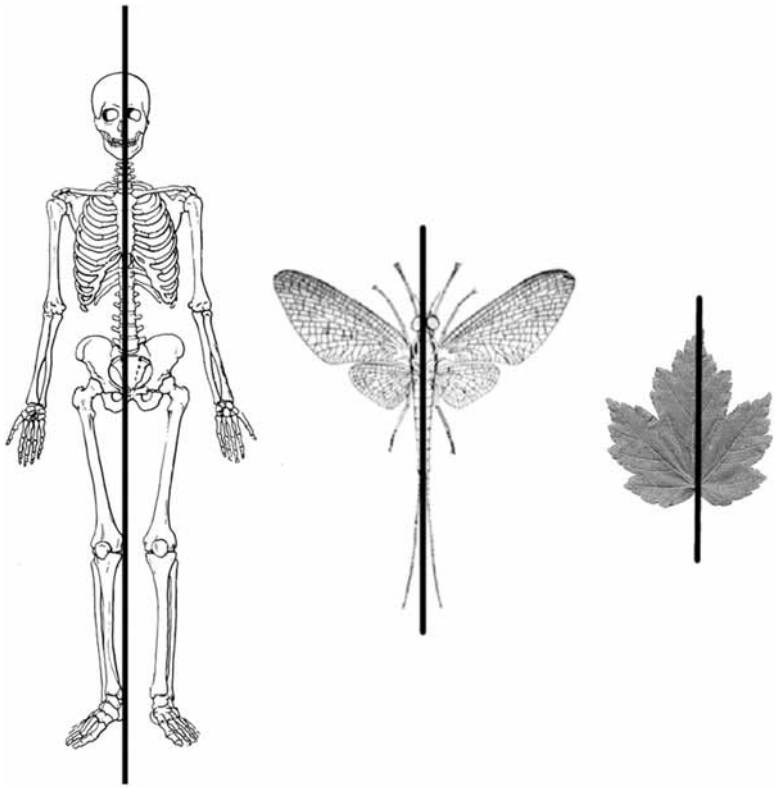

Figure 1. Examples of organisms showing symmetry along a midline plane. The wings of the mayfly are an example of "matching symmetry," where symmetry is observed in separate bilateral structures. The leaf is an example of "object symmetry," where symmetry is seen within a single structure centered on a midline plane. The human skeleton is composed of anatomical units showing both matching symmetry (e.g., upper and lower limbs) and object symmetry (e.g., skull, vertebrae).

McAdams and Arkin, 1997). *Developmental stability* is the suppression of phenotypic variation within individuals and refers to the capacity for developmental trajectories to resist accidents and perturbations during growth.

In the comparative studies of right and left sides of an organism, the underlying developmental assumption is that organisms possess some sort of homeostatic mechanisms that control the development of traits that occur bilaterally (Van Valen, 1962). These mechanisms, though poorly understood, determine the organism's developmental stability. According to Klingenberg (2002), developmental noise can cause differences between body sides. These responses are mediated by the organism's DI, defined as the organism's

tendency to produce a morphological change in response to developmental perturbations. Developmental instability and developmental stability are, therefore, two sides of the same coin; the former referring to the organism's phenotypic response to perturbations, the latter to the organism's capacity to buffer these insults through homeostatic mechanisms that inhibit the expression of a phenotypic response (Klingenberg, 2003). Many questions about these homeostatic mechanisms remain unanswered, and little is known about the developmental basis for asymmetry.

Though departure from symmetry is a property of the individual, patterns of asymmetry in a particular trait are studied at the level of the population or sample (Palmer, 1994). When departure from symmetry is quantified as the difference between similar measures on the left and right sides (L–R) in a population, three basic types of asymmetry are defined on the basis of the frequency distribution of the (L–R) measure. Small, subtle deviations from perfect symmetry, which do not show a tendency to a specific side (nondirectional), characterize FA. The pattern of L–R symmetry in a sample of individuals exhibiting FA, shows a unimodal distribution with a mean of zero and with variation symmetrically distributed around the mean (Figure 2a). Evidence for a positive correlation between FA and DI comes from the results of studies that show FA to increase as environmental and/or genetic "stress" increases (Møller and

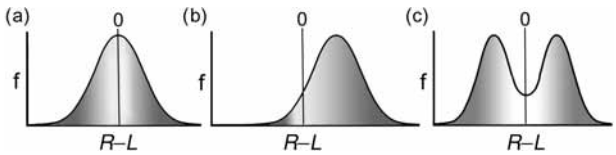

Figure 2. Asymmetry may be characterized by the distribution of asymmetry values within a population (after Palmer and Strobeck, 1986; Van Valen, 1962). In this figure, "asymmetry" is quantified as the signed arithmetic difference between right and left measurements ($L-R$) of a single dimension. (a) In *fluctuating asymmetry*, deviations from symmetry are small and randomly distributed as to side, so the distribution of $L-R$ is unimodal and centered at zero. This definition assumes that the underlying "ideal" form is perfectly symmetric (i.e., $L-R=0$). (b) *Directional asymmetry* describes a measurement that is generally larger on the same side in all members of a population, and the mean value is something other than zero ($L-R\neq 0$). (c) *Antisymmetry* refers to a measurement that is usually asymmetric, but larger on the right in some individuals, and larger on the left in others. In this case, the distribution of ($L-R$) is bimodal or platykurtic (adapted from Palmer, 1994).

Swaddle, 1997; Palmer and Strobeck, 1992; Zakharov, 1992), but others argue that the relationship between FA and DI is weak (Fuller and Houle, 2002). *Directional asymmetry* (DA) describes a pattern where the difference between sides is biased as to side (i.e., one side tends to be consistently larger across individuals in a population). An example of DA occurs in the bill of the wry-billed plover (*Anarhynchus frontalis*), which is always bent to the right at the tip by up to 12° (Neville, 1976). DA need not favor a single side for all characters within an organism, but can favor the left side for some traits and the right side for different traits. Distributions for characters showing DA in a population are unimodal with a mean that is different from (either greater or less than) zero (Figure 2b). *Antisymmetry* describes a pattern of bilateral variation in a sample where the difference between sides is consistent, but nondirectional. A common example is the fiddler crab (*Uca pugnax*) where the crusher claw is always larger than the cutter claw, but it is just as likely that the right claw be the crusher claw as it is that the crusher claw be on the left. Because the left or the right side may be predominant in cases of antisymmetry, the distribution that describes antisymmetry in a sample is bimodal and centered on zero (Figure 2c).

Since we are interested in DI as a basis for the production of the DS phenotypes, this study is concerned with FA. Most simply, FA can be thought of as a metric that compares corresponding measures from the right and left sides of organisms within a sample. Most analyses aim to determine whether or not differences in the magnitude of FA exist in two samples. Although our ultimate goal is to understand the development of phenotypes in humans with DS, humans provide a less than ideal study subject since genetic background cannot be controlled and collection of data from certain developmental time points is not possible. To our advantage, several informative mouse models for DS have been developed (Davisson et al., 1993; Sago et al., 1998) and are useful in the study of DI in aneuploidy as demonstrated by FA.

THE QUANTITATIVE STUDY OF FA

The use of FA as an indicator of increased levels of DI has been broadly reviewed (e.g., DeLeon, 2004; Møller and Swaddle, 1997; Polak, 2003). Traditional methods for studying FA were described fully by Palmer (1994). Superimposition for the purpose of studying asymmetry was briefly introduced by Bookstein (1991: 267–270) and applied in a more fully developed context by Auffray et al. (1996). The Procrustes approach was later revised by

Smith et al. (1997), thus formally linking the study of FA with geometric morphometrics (see Bookstein, 1991; Marcus et al., 1996; Richtsmeier et al., 1992, 2002a for reviews of geometric morphometrics). The Procrustes approach to FA was extended by Klingenberg and McIntyre (1998) to a two-factor ANOVA design for the purpose of estimating and testing the different components of asymmetry. Mardia et al. (2000) elaborated on the formal statistics of symmetry of shapes using Procrustes superimposition.

Procrustean approaches fall within the class of geometric morphometrics called superimposition methods (Richtsmeier et al., 2002a). Superimposition methods involve the translation, rotation, and scaling of landmark data from two or more objects into the same coordinate space according to a specified rule. With two objects, one object is designated as the "reference," and the other is designated as the "target." The displacements necessary to take the landmarks in the reference to their new locations in the superimposed target are used to characterize the differences between the two landmark sets. With more than two objects, variation in form is described relative to the iteratively computed sample mean.

We have chosen to develop an alternate approach to the study of asymmetry for the following reasons. When using Procrustes, the researcher chooses a particular criterion for superimposing the two sides. For example, the least-squares criterion (where, after reflection, the forms are superimposed so that the sum of the squared distances between corresponding landmarks on the two forms are minimized) leads to the Generalized Procrustes superimposition. This is currently the most commonly used strategy for superimposition (Klingenberg et al., 2002). Alternatively, the generalized resistant fit algorithm (Chapman, 1990; Rohlf and Slice, 1990; Siegel and Benson, 1982) uses repeated medians to calculate the best fit between two mean forms and attributes differences to a small number of landmarks, instead of spreading it over the whole object, as is done using the least-squares approach. The use of different fitting criteria for matching gives different superimpositions (Richtsmeier et al., 2002a; Rohlf and Slice, 1990). This means that localized differences between two objects or the local measures of variation among objects in a sample will vary depending upon the superimposition criterion used. Results are, therefore, affected by the scientist's arbitrary choice of a superimposition criterion. The choice of superimposition criteria is rarely consciously made by the researcher, but instead is integrated into the software program. The crucial point is that the superimposition scheme used in analysis can change results of an analysis

by shifting the location of maximum differences from one biological location to another, or spread the effects of a shifted biological locus to unaffected, neighboring biological loci. Moreover, the data cannot inform us of which superimposition is the correct one (Richtsmeier et al., 2002b).

What follows statistically from these observations is that, due to the nuisance parameters of rotation and translation, neither the mean nor the variance–covariance matrix can be estimated consistently from data using Procrustes. Lele and Richtsmeier (1990) first recognized this problem. It was further explained by Lele (1991, 1993) and proven mathematically by Lele and McCulloch (2002). Walker (2001) published similar findings. If the variance–covariance structure cannot be estimated correctly using Procrustes, the development of models that decompose Procrustes variance structures in order to separate components of symmetric variation among individuals from that within individuals seems ill-advised.

AN ALTERNATE APPROACH TO THE ASSESSMENT OF FA

Our approach to the study of FA is based on Euclidean distance matrix analysis (EDMA; Lele and Richtsmeier, 2001). Suppose we have an object that is described by a collection of landmarks in three dimensions. In contrast with most other landmark-based morphometric methods, EDMA does not require placement of the observations under study into an arbitrary coordinate system in order to describe or compare them. Instead the coordinate data are rewritten as a matrix of interlandmark distances. These distances remain the same, no matter how the objects are positioned or oriented. This property is called *coordinate-system invariance* (Lele and McCulloch, 2002; Lele and Richtsmeier, 2001).

Before we can study FA in a sample, we must first be able to describe DA, because measurement of the former is dependent on the latter. Our algorithm for the analysis of DA is described in terms of a single, left–right pair of linear distance between landmarks. However, the steps of the algorithm are applied to every left–right distance pair. For each individual in a sample, a form matrix is computed, consisting of all unique interlandmark distances. The linear distances that occur bilaterally are paired, one being from the left side of the organism (L) and other from the right (R). For each individual i, we define the (signed) asymmetry of a distance pair as $(L–R)_i$. If $(L–R)_i = 0$, then individual i

is perfectly symmetric for that pair of distances. Asymmetric individuals will either have $(L-R)_i > 0$ or $(L-R)_i < 0$, depending on which side is larger. The *sample distribution* of $(L-R)$ contains information about both DA and FA. The mean of the sample, $\overline{(L-R)}$, measures DA. The amount of dispersion (variation) in the sample (the measurement of which is described below) is a measurement of FA.

Our bootstrap-based algorithm for measuring DA was developed by Cole (2001) and is an extension of work by O'Grady and Antonyshyn (1999). Programs are available from the Richtsmeier laboratory website: http://oshima.anthro.psu.edu. The approach is reviewed briefly here. Again, for the sake of clarity, we are describing the algorithm in terms of a single pair of left–right distances. However, in practice, the bootstrapping procedure is not applied independently to each distance pair. Instead, entire individuals (i.e., with linear distances calculated from the complete set of landmarks used in the study) are resampled randomly and with replacement, so that information about the covariances among measurements is retained in the data.

Preliminary step: We describe the DA in a sample for each linear distance pair by calculating the mean of (*L*–*R*), calling it $\overline{(L-R)}$. If this mean were exactly zero, then the sample would be symmetric *on the average*, even though each of the individuals in the sample might be asymmetric to some degree. In such a case, there would be no DA for the sample. However, if $\overline{(L-R)}$ were, in fact, different from zero (and it would be likely to be at least slightly different for any real sample), we would then want to know how far it must be from zero before we would consider the DA in the sample to be significant. To determine this, we use the remainder of the algorithm to construct a confidence interval for $\overline{(L-R)}$ using the bootstrap.

Step 1: Denote the size of sample X as n_X. Construct a bootstrap *pseudosample*, called X*, by selecting n_X individuals from X randomly and with replacement. This is a typical resampling strategy for nonparametric bootstrapping (Davison and Hinkley, 1997; Efron and Tibshirani, 1993). Use this pseudosample to compute a *bootstrap estimate* of the mean asymmetry, calling it $\overline{(L-R)}^*$.

Step 2: Repeat Step 1 M times where M is some large number (e.g., 1,000 or more) generating a new random pseudosample each time. The result is a distribution of M estimates of $\overline{(L-R)}^*$, the pseudosample means.

Step 3: Sort the vector of M bootstrap estimates of $\overline{(L-R)}^*$ in ascending order: $\overline{(L-R)}_{[1]} \ldots \overline{(L-R)}_{[M]}$. Truncate the sorted vector to obtain a bootstrap estimate of the marginal confidence interval for $\overline{(L-R)}$. For a $100(1-\alpha)\%$ confidence interval, the lower bound will be $\overline{(L-R)}^*_{[(M)(\alpha/2)]}$ and the upper bound will be $\overline{(L-R)}^*_{[(M)(1-\alpha/2)]}$. For example, when $M = 1{,}000$ and 90% confidence intervals are desired (where $\alpha = 0.10$), the estimates of the lower and upper bounds will be $\overline{(L-R)}^*_{[50]}$ and $\overline{(L-R)}^*_{[950]}$, respectively. This method for obtaining a confidence interval by truncating a sorted vector of bootstrap estimates is called the percentile method (Davison and Hinkley, 1997; Efron and Tibshirani, 1993).

Step 4: Evaluate the DA of the sample by determining whether the confidence interval includes zero, which is the expected value of $\overline{(L-R)}$ when there is no DA. If the interval *excludes* zero, then the null hypothesis is rejected, and we conclude that there is a significant degree of DA—a "handedness"—in the sample as a whole for the distance being considered.

If significant DA is found for one or more linear distance pairs, we must decide whether the *biological* interpretation of DA should be a part of the analysis. For some studies, an understanding of DA patterns may be of primary importance. For example, our original application of EDMA to the study of asymmetry (Cole, 2001) was a study of children affected with unilateral coronal craniosynostosis (a problem of antisymmetry, although it was treated as DA problem after reflections of some observations in the sample; Figure 3). In this case, we were interested not only in identifying which specific distances were asymmetric (as the result of premature suture fusion), but also in identifying the "handedness" of each asymmetric distance (relative to the side of suture fusion). However, if there is no rationale for a biological investigation of DA, we might consider DA to be a nuisance that confuses our measurement of FA. Whether the DA in a measurement is significant or not, it must be accounted for before FA can be accurately measured (Palmer and Strobeck, 1986). Otherwise, we run the risk of confusing FA and the "total" asymmetry in a sample.

There are many different ways to quantify FA in paired distances (e.g., Palmer and Strobeck, 1986). One simple way is to express the asymmetries of individuals as absolute deviations from the sample mean. To simplify further discussion, we introduce additional notation. Let us use A_i to represent the absolute value of the difference of individual i's left–right asymmetry from the

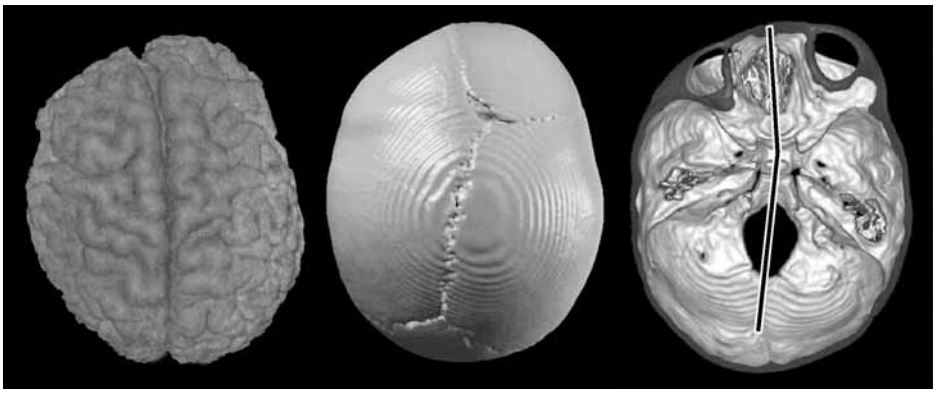

Figure 3. An example of DA where the midline is directly and visibly affected. This figure shows a superior view of (from left to right) the neural surface of the brain, the superior surface of the neurocranium, and the endocranial base with a line showing the midsagittal plane of an individual with premature closure of the left coronal suture. Although asymmetry of midline structures is obvious in this case, the potential for direct effects of asymmetry on midline points should not be ignored in analyses of fluctuating asymmetry.

sample mean:

$$A_i = \left|(L-R)_i - \overline{(L-R)}\right|$$

Because $\overline{(L-R)}$ represents a measure of DA for the sample, the distribution of A is a measure of the amount of FA for the sample (i.e., the subtraction of $\overline{(L-R)}$ means that the directional-asymmetry component of the total asymmetry has been removed).

We now present our algorithm for comparing levels of FA in two samples. Our null hypothesis is that there is no difference between samples in the amount of FA. This algorithm is similar to the DA algorithm in that it uses the bootstrap.

Preliminary step: Suppose we are comparing two samples called X and Y. Calculate the $L-R$ means for both samples, calling them $\overline{(L-R)}_{\mathrm{X}}$ and $\overline{(L-R)}_{\mathrm{Y}}$, respectively. For sample X, calculate the A statistic for each individual in the sample. Recall that $A_i = \left|(L-R)_i - \overline{(L-R)}\right|$ and that this is calculated for each distance pair. Calculate the sample mean and call it $\overline{A}_{\mathrm{X}}$. Similarly, calculate the sample mean of A for sample Y, calling it $\overline{A}_{\mathrm{Y}}$. These means are measures of FA within their respective samples, with larger values of A indicating greater degrees of asymmetry. Our null hypothesis is that the amount of FA is the same in the two samples, or H_0: $\overline{A}_{\mathrm{X}} - \overline{A}_{\mathrm{Y}} = 0$. We can give the difference in means

a new name, D. We use the bootstrap to construct a confidence interval that will determine whether D is significantly different from zero. This is an application of Hall and Martin's (1988) bootstrap-based two-sample test.

Step 1: Denote the size of sample X as n_X. Similarly, denote the size of sample Y as n_Y. As with the DA algorithm, we will use a nonparametric bootstrap approach to resampling. Construct a bootstrap pseudosample called X* by sampling n_X individuals from X randomly and with replacement. Similarly, construct a pseudosample called Y* by sampling n_Y individuals randomly and with replacement from Y. Compute the means of A from the bootstrap samples and call them $\overline{A}_X{}^*$ and $\overline{A}_Y{}^*$. Then call the differences in bootstrap means, $D^* = \overline{A}_X{}^* - \overline{A}_Y{}^*$.

Step 2: Repeat Step 1 M times where M is some large number (e.g., 1,000 or more), generating new random pseudosamples each time. The result is a vector of M bootstrap estimates (D^*) for the difference between sample means (D).

Step 3: Sort the M bootstrap estimates of D in ascending order: $D^*_{[1]} \ldots D^*_{[M]}$. Truncate the vector to obtain $100(1-\alpha)\%$ confidence intervals, as described above for the DA algorithm.

Step 4: If the bootstrap confidence interval for D excludes zero, we reject the null hypothesis and conclude that there is a significant difference in the amount of FA in the two samples. If the null hypothesis is rejected and $D = \overline{A}_X - \overline{A}_Y > 0$, we conclude that there is a greater amount of FA in sample X. Conversely, if the null hypothesis is rejected and $D < 0$, we conclude that there is a greater amount of FA in sample Y.

This algorithm may be applied in cases of both "matching" and "object" symmetry (Mardia et al., 2000). For matching symmetry, where there are no landmarks that belong to the midline plane by definition (e.g., insect wings), we examine asymmetry in all possible distances that are present bilaterally. Because we are using interlandmark distances, our measurements of asymmetry are coordinate-system invariant and are not affected by arbitrary locations or orientations of the left- and right-side structures. For "object" symmetry, there may be landmarks that lie in the midline plane by definition (e.g., midsagittal landmarks on the skull; see Figure 3). With our approach, we can include these landmarks if appropriate. The inclusion of midline landmarks allows us to examine asymmetry in bilateral distances that have midline landmarks at one end. We do not consider distances *between* midline landmarks in our analyses because

they are not paired. Note that our method makes no assumptions about the midline points being coplanar; information about any distortion in the midline plane will be contained in comparisons of all the bilateral distances. As with considerations of matching symmetry, our use of interlandmark distances ensures coordinate-system invariance so that the orientations and positions of the individual observations do not affect the results.

Finally, we should mention that there is another potential factor that can confuse our consideration of FA, particularly in comparisons between samples: variation in scale (Palmer and Strobeck, 1986). Suppose we are studying a sample of humans affected with a particular genetic disorder, and we want to compare the degree of FA in these humans with a genetically engineered mouse model of the same disorder (e.g., DS). Because measurements of human skulls are absolutely much larger than the corresponding measurements on the skulls of mice, we would expect the $\overline{A}$ statistics to be larger in humans, even if the actual degree of FA is the same. This is because of the well-known positive association between the means and variances of linear distances (Lande, 1977; Palmer and Strobeck, 1986). If we want to compare levels of FA in samples of organisms that differ substantially in size, we need to incorporate a scale-adjustment, so that we will explicitly examine *relative* FA. Further discussion of this problem, along with some proposed solutions, is found in Palmer and Strobeck (1986).

COMPARATIVE ANALYSIS OF FA IN ANEUPLOIDY

Using Animal Models to Study DS

As noted previously, two distinct schools of thought have emerged to explain why the inheritance of three copies of Chr 21 genes results in disruption of normal patterns of development. The *amplified DI* hypothesis holds that the correct balance of gene expression in pathways regulating development is disrupted by dosage imbalance of the hundreds of genes on Chr 21 (Shapiro, 1975, 1983, 1999, 2001). Support for this hypothesis includes: (a) the observation that features seen in DS are nonspecific, occurring in other trisomic conditions (Hall, 1965; Shapiro, 1983) and in the population at large (albeit at much lower frequency); and (b) measures of significantly increased individual phenotypic variation among individuals with Ts21 compared to euploid individuals (Kisling, 1966; Levinson et al., 1955; Roche, 1964, 1965; Shapiro, 1970). The amplified DI hypothesis states that DS phenotypes, and the increased variation

noted in DS populations, result from a disruption of an evolutionarily achieved balance of genetic programs regulating development and recognizes that pathways disrupted by Ts21 involve many more genes than those on Chr 21 (Reeves et al., 2001).

The other ideas proposed to explain why Ts21 disrupts normal patterns of development are summarized by the *gene dosage effects* hypothesis that argues for a more specific relationship between particular genes and specific individual DS traits (Delabar, 1993; Korenberg et al., 1994). The gene dosage effects hypothesis holds that dosage imbalance of a specific gene or small group of genes from Chr 21 is responsible for specific individual DS traits.

It is clear that the debate surrounding these hypotheses (Pritchard and Kola, 1999; Reeves et al., 2001; Shapiro, 1999) cannot be resolved by continued study of adult DS individuals. A joint focus on the mechanism of gene action (e.g., Saran et al., 2003) and the phenotypic consequences for development is needed to understand the etiology of this complex disorder. A comprehensive explanation of the etiology of DS features should consider *developmental* consequences of aneuploidy and not only the direct overexpression of the triplicated genes or the phenotypic consequences of this overexpression as manifest in the adult (Reeves et al., 2001). Since the biological processes underlying these two hypotheses and the data needed to sufficiently test them cannot be evaluated using human data, experimental organisms are required. Mouse strains with segmental trisomy 16 have been studied as genetic models of DS (Baxter et al., 2000; Davisson et al., 1993; Neville, 1976; Reeves et al., 1995; Richtsmeier et al., 2000; Sago et al., 1998, 2000). Ts1Cje is a segmental trisomy 16 model that arose as a fortuitous translocation of mouse Chromosome 16 (Chr 16) in a transgenic mouse line (Sago et al., 1998). These mice are at dosage imbalance for a segment of mouse Chr 16 corresponding to a human Chr 21 region that spans 9.8 Mb and contains 79 of the 225 genes in the Chr 21 gene catalog (Hattori et al., 2000). The genetic insult in Ts1Cje mice and in another segmental trisomy 16 model, Ts65Dn, has been shown to correspond closely to that of segmental Ts21 in human beings (Reeves et al., 1995; Sago et al., 2000). Although species differences need to be kept in mind when complex characters are compared in mouse and human, a detailed, three-dimensional analysis of the skull of segmentally trisomic mice and their normal littermates demonstrated direct parallels between the human DS craniofacial phenotype and that of the Ts1Cje and Ts65Dn mouse skull (Richtsmeier et al., 2000, 2002b). When compared statistically to the skulls of normal littermates,

the segmentally trisomic Ts65Dn and Ts1Cje craniofacial skeletons showed an overall reduction in size, a disproportionately reduced midface, maxilla and mandible, and reduced interorbital breadth. Since the effects of gene dosage imbalance on conserved genetic pathways are expected to be similar in mice and human beings, mice with segmental trisomy provide the experimental basis to investigate corresponding developmental processes disrupted by the analogous trisomy in mouse and human. Analysis of prenatal mice is ongoing (Richtsmeier et al., 2002c, 2003).

Analysis of FA in Aneuploid and Euploid Ts1Cje Mice

If differences in developmental stability between euploid and aneuploid mice are the basis for, or contribute to, the craniofacial anomalies of development previously quantified, then differences in the measures of FA should also be evident in a comparison of the euploid and aneuploid samples. Moreover, if aneuploidy results from amplified DI, we predict that measures of FA should be increased in aneuploid as compared to euploid mice. The analysis presented here uses three-dimensional coordinates of landmark data collected using the Reflex microscope from adult, segmentally trisomic Ts1Cje mice ($N = 15$) and unaffected littermates ($N = 12$) (Figure 4). Landmarks collected multiple times from each specimen were 27 in number. Measurement error studies were done following details given previously (Richtsmeier et al., 1995). When it was determined that measurement error was minimal and comparable to previous studies using the Reflex microscope (Richtsmeier et al., 2000), an average was computed from two data collection trials.

As noted by Palmer and Strobeck (1986) and Palmer (1994), the calculation of FA is particularly sensitive to measurement error. The method we present here does not, as yet, include an integrated test of FA over measurement error. This may be important because measurement error can contribute directly to measures of FA and can be responsible, at least in part, for differences in FA between measures and between samples. Because the data sets used here were initially collected to study difference in shape, we estimated the precision of each landmark separately. Precision refers to the average absolute difference between repeated measures of the same individual (Kohn and Cheverud, 1992). Three-dimensional coordinates of landmarks were collected several times from 10 mouse skulls with the skull remaining in the same position for each trial. The average variance along the x, y, and z axes for all landmarks

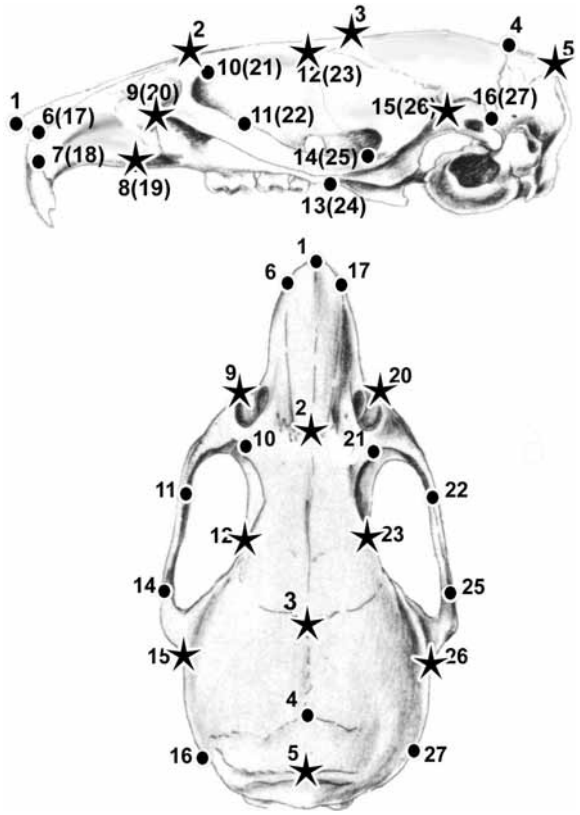

Figure 4. Schematic views of the mouse cranium (upper panel: lateral view; lower panel: superior view) showing landmarks collected using the Reflex microscope. Landmark number and label are given. For bilateral landmarks, the number of the right-sided landmark is shown in parentheses on the lateral view. Landmarks marked by a star were used as an endpoint for linear distances used in the current analysis of FA. *Cranial landmarks*: 1, nasale; 2, nasion; 3, bregma; 4, intersection of parietal and interparietal bones; 5, intersection of interparietal and occipital bones at the midline; 6(17), anterior-most point at intersection of premaxillae and nasal bones; 7(18), center of alveolar ridge over maxillary incisor; 8(19), most inferior point on premaxilla–maxilla suture; 9(20), anterior notch on frontal process lateral to infraorbital fissure; 10(21), intersection of frontal process of maxilla with frontal and lacrimal bones; 11(22), intersection of zygomatic process of maxilla with zygoma (jugal), superior surface; 12(23), frontal–squamosal intersection at temporal crest; 13(24) intersection of maxilla and sphenoid on inferior alveolar ridge; 14(25), intersection of zygoma (jugal) with zygomatic process of temporal, superior aspect; 15(26) joining of squamosal body to zygomatic process of squamosal; 16(27) intersection of parietal, temporal, and occipital bones.

ranged from 0.002–0.061 mm. Further refinements of the method presented here will include integrated measures of FA and measurement error.

From the group of all possible linear distances among the landmarks, we used 18 paired distances to determine if the degree of FA is increased in aneuploid mice. Distances were chosen on the basis of their contribution to significant cranial dysmorphology in Ts1Cje mice (Richtsmeier et al., 2002a). Mean directional asymmetries were computed for left- and right-paired distances in the aneuploid and euploid Ts1Cje samples (X_i and Υ_i), and the between-sample difference between measures of absolute asymmetry, A_i, were calculated for corresponding linear distances. As stated previously, the null hypothesis is that for each measure, the two samples show similar magnitudes of absolute asymmetry. Therefore, the expected value of the between-sample difference for measures of absolute asymmetry for corresponding linear distances is zero. In our application, the measure of absolute asymmetry for each linear distance in the euploid sample was subtracted from the corresponding measure in the aneuploid sample, so that values > 0 indicate greater asymmetry in the aneuploid sample for a given distance, while values < 0 indicate greater asymmetry in the euploid sample. The measures of A_i for each sample are given in Figure 5.

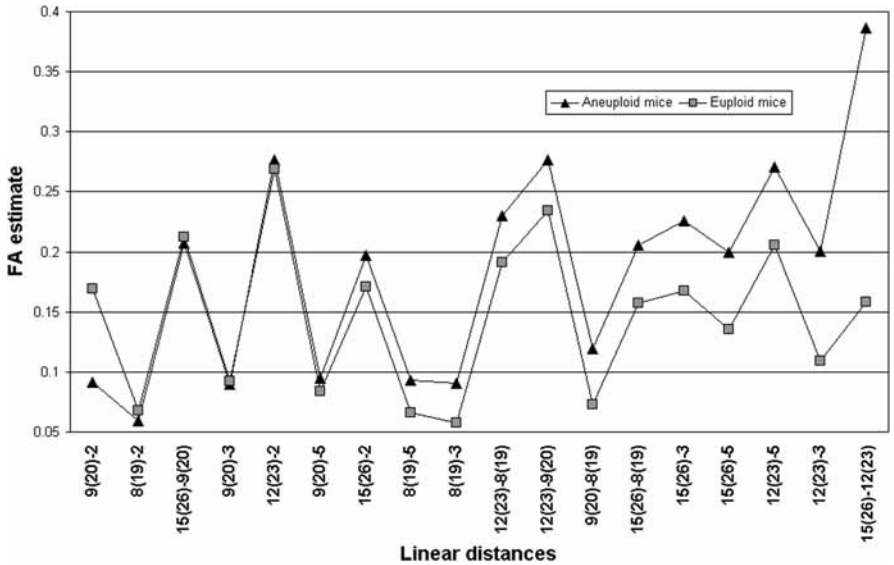

Figure 5. Estimates of mean FA ($\bar{A}_i$ as described in the text) for the samples of aneuploid and euploid Ts1Cje adult mouse crania for linear distances between landmarks given in Figure 4. Landmarks on the right side of the skull are given in parentheses.

Figure 6 provides a summary of the difference in means, D, for all linear distances considered in the Ts1Cje mouse model for DS. Fourteen of the 18 paired linear distances indicate a larger degree of asymmetry in the aneuploid sample ($D_i > 0$ on the right of Figure 6), two show approximately equal measures of asymmetry in the two samples, and two linear distances show a higher degree of FA in the euploid Ts1Cje sample ($D_i < 0$ on the left side of Figure 6). Remember that the distribution of D is a measure of difference in FA for the sample, because the DA component of total asymmetry has been removed in a previous step of the algorithm. Of those linear distances that indicate a larger degree of asymmetry in the aneuploid sample, confidence interval testing shows that four of these differences are significant (marked by arrows on Figure 6). None of

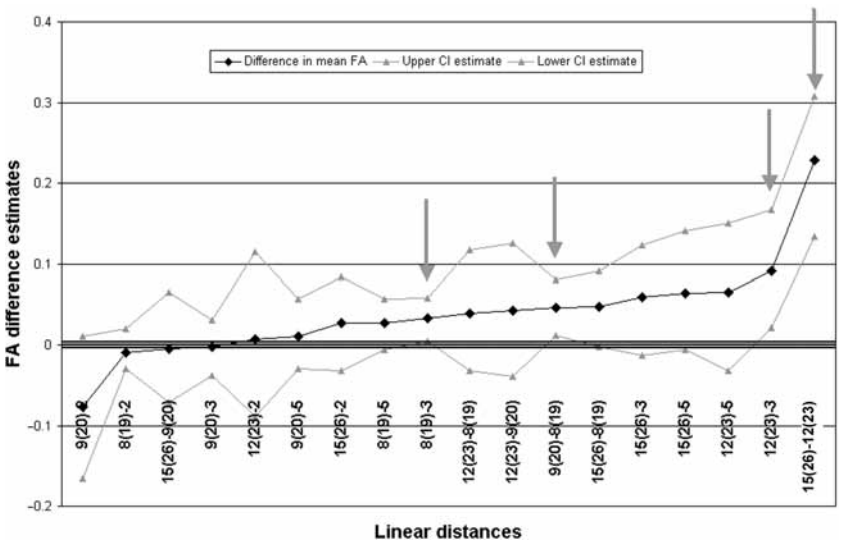

Figure 6. Graph of comparison of measures of FA in aneuploid and euploid Ts1Cje mice. The y-axis is the measure of the difference in absolute asymmetries between aneuploid and euploid samples for all linear distances considered. The x-axis represents the 18 paired linear distances. Linear distances are defined by the landmarks used as endpoints; landmarks on the right side of the skull are given in parentheses. The estimates of the difference in FA between the two samples are shown as black diamonds. Estimates of the lower and upper bounds of the confidence interval ($\alpha = 0.10$; 1,000 resamples) for each linear distance appear as gray triangles. Those measures of difference in fluctuating asymmetry that show a significant difference in asymmetry in the euploid and aneuploid sample (i.e., 0 is not included in the confidence interval) are marked with a gray arrow.

the measures that are more asymmetric in the euploid sample are shown to be significant by confidence interval testing.

When these results are used to identify the anatomical locations that show significant differences in FA between aneuploid and euploid samples, certain landmarks are shown to be involved more frequently than others (Figure 7). Landmarks that contribute disproportionately to a greater degree of asymmetry in the trisomic mice are located on the intersection of the premaxilla and maxillary bones (landmarks 8 and 19) and the neurocranium at bregma (landmark 3). Overall increased FA in the Ts1Cje aneuploid skull is not limited to a specific

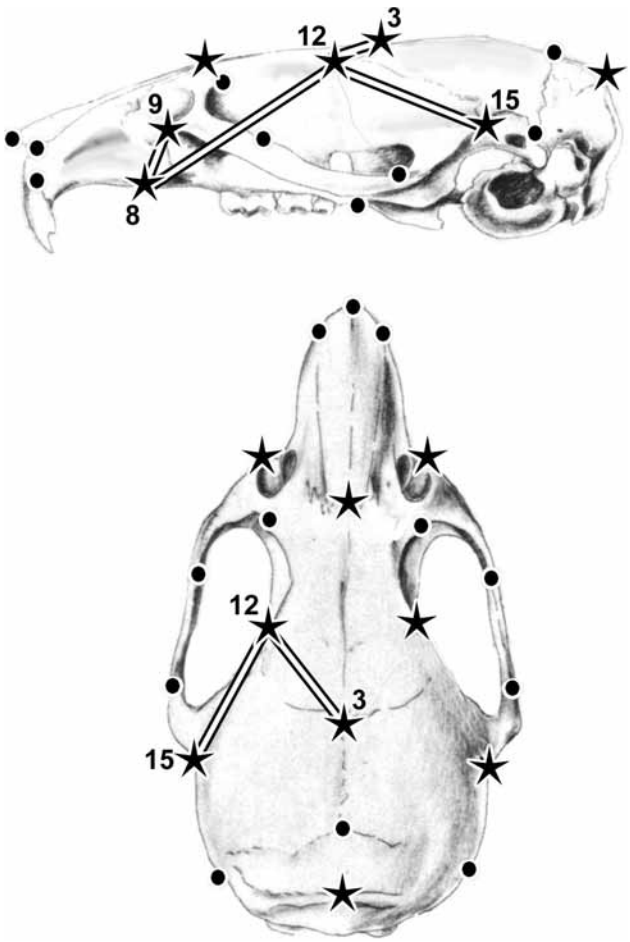

Figure 7. Graphic depiction of those linear distances shown by confidence intervals (see Figure 6) to be relatively more asymmetric in the aneuploid sample are depicted on one side of the skull only.

bone or functional unit of the skull, but is distributed across the skull. Further tests of the significance of the contribution of specific landmarks to FA can be conducted following methods for the detection of influential landmarks outlined by Lele and Richtsmeier (1992).

A previous comparison of the skulls of Ts1Cje euploid and aneuploid mice (Richtsmeier et al., 2002b) found that the Ts1Cje aneuploid mice have a relatively shorter skull along the rostro-caudal axis, with the primary reduction being located on the bones of the face (i.e., premaxilla, maxilla, anterior frontal) and a marked reduction in interorbital distance. The Ts1Cje aneuploid neurocranium was also reduced along the mediolateral axis, but to a lesser degree. Localization of the linear distances that show significantly increased FA in the aneuploid sample (Figure 7) indicates increased FA local to the premaxilla and maxilla of the aneuploid mouse—an area that was shown previously to be significantly dysmorphic in Ts1Cje. However, linear distances on the neurocranium that show statistically significant increased FA in the aneuploid sample in this study were not previously identified as significantly different when compared to their euploid littermates (Richtsmeier et al., 2002b).

As discussed previously, two viable, though not mutually exclusive, hypotheses have been proposed to explain the phenotypes associated with trisomy. We suggested earlier that if increased DI were the cause of dysmorphic features of the skull in Ts1Cje mice, then measures of FA should be increased in aneuploid mice relative to their euploid littermates. We have found some support for this hypothesis in that a majority (78%) of linear distances show higher values of FA in aneuploid mice, though only four of these measures (28%) are significant. However, these linear distances do not correspond with measures of shape that were previously shown to be significantly different from normal (Richtsmeier et al., 2002b).

To fully test the amplified DI hypothesis, an increased understanding of the processes that underlie DI is required coupled with additional analyses using larger sample sizes and additional age groups. Unpublished analyses of morphological integration of Ts1Cje and Ts65Dn mice, find that crania and postcrania of the adult aneuploid mice show *increased* morphological integration as compared to their normal littermates (Hill et al., 2003; Richtsmeier et al., 2002c, 2003). Although only a conjecture at this point, we can envision a developmental scenario where gene action in aneuploidy affects cellular processes in such a way that localized phenotypic dysmorphology of the skeleton results. This dysmorphology may be subtle, but significant enough that

developmental adjustments need to be made to ensure adequate structural stability and proper function. The adjustments could include regions that are not directly affected by dysmorphogenesis. The result is a predictable phenotype composed of localized areas of heightened dysmorphology that can be characterized according to a quantifiable distribution. The phenotypic targets of dysmorphogenesis and the adjustments that need to be made in adjoining tissues combine to produce a typical phenotype (like the characteristic DS facial appearance) that manifests itself at the individual level as a "characteristic" phenotype, but at the population level as one of increased phenotypic variability. The increased variability comes from both the actual distribution of effects on localized structures and the requisite and customized adjustments made by adjoining tissues in response to the primary dysmorphology. If the processes responsible for impacting skull growth in trisomy operate in ways similar to what is described above, this could explain the combined findings of increased phenotypic variability, increased morphological integration, and localized increases in FA in samples of aneuploid mice. Theory and methods from evolutionary biology that account for the coordination of developmental modules (e.g., Klingenberg, 2003; Wagner, 1995) will be useful in the evaluation of these ideas.

SUMMARY AND CONCLUSIONS

We have presented a novel method for statistical comparison of FA. The advantages of our method include:

1. the straightforward inclusion of three-dimensional data;
2. the lack of superimposition, so that the user does not need to arbitrarily select a fitting criterion;
3. identification of significant differences in FA by bootstrap confidence intervals;
4. presentation of local measures of FA, enabling identification of the affected anatomical structures and the proposal of testable developmental hypotheses.

The results of our analysis of FA in the Ts1Cje mouse provide preliminary support for the amplified DI hypothesis and provide the basis for a model of the

interplay of dysmorphology and FA in aneuploidy that can be further explored in studies of development.

ACKNOWLEDGMENTS

Programs for the EDMA approach to FA are available for free download from http://oshima.anthro.psu.edu (Richtsmeier lab website) and from http://3dlab.umkc.edu (Cole lab website). We thank our collaborators Roger H. Reeves and Charles J. Epstein for providing animals for this research. Ann Zumwalt collected some of the landmark data. Kristina Aldridge prepared figures 1, 2, 3, 6, and 7. We thank Dennis Slice for inviting us to contribute to this volume and for his efforts in bringing these papers together. This presentation was greatly improved and clarified due to helpful comments provided by Dennis Slice, Kristina Aldridge, and an anonymous reviewer. This work was supported in part by NSF-SBER004903; PHS awards F33DEO5706, P60 DE13078, HD 24605, HD 38384, and HD 34198.

REFERENCES

Antonarakis, S. E., 1991, Parental origin of the extra chromosome in trisomy 21 as indicated by analysis of DNA polymorphisms. Down Syndrome Collaborative Group, *N. Engl. J. Med.* 324:872–876.

Antonarakis, S. E., Petersen, M. B., McInnis, M. G., Adelsberger, P. A., Schinzel, A. A., Binkert, F. et al., 1992, The meiotic stage of nondisjunction in trisomy 21: Determination by using DNA polymorphisms, *Am. J. Hum. Genet.* 50:544–550.

Antonarakis, S. E., Avramopoulos, D., Blouin, J. L., Talbot, C. C., Jr., and Schinzel, A. A., 1993, Mitotic errors in somatic cells cause trisomy 21 in about 4.5% of cases and are not associated with advanced maternal age, *Nat. Genet.* 3:146–150.

Auffray, J.-C., Alibert, P., Renaud, S., Orth, A., and Bonhomme, F., 1996, Fluctuating asymmetry in *Mus musculus* subspecific hybridization: Traditional and Procrustes comparative approach, in: *Advances in Morphometrics*, L. Marcus, M. Corti, A. Loy, G. J. P. Naylor, and D. E. Slice, eds., Plenum Press, New York, pp. 275–283.

Baxter, L. L., Moran, T. H., Richtsmeier, J. T., Troncoso, J., and Reeves, R. H., 2000, Discovery and genetic localization of Down syndrome cerebellar phenotypes using the Ts65Dn mouse, *Hum. Mol. Genet.* 9:195–202.

Bookstein, F., 1991, *Morphometric Tools for Landmark Data: Geometry and Biology*, Cambridge University Press, Cambridge.

Chapman, R., 1990, Conventional Procrustes approaches, in: *Proceedings of the Michigan Morphometrics Workshop*, F. J. Rohlf and F. L. Bookstein, eds., University of Michigan Museum of Zoology, Ann Arbor, pp. 251–267.

Cole, T. M. III, 2001, Chapter 7. Further applications of EDMA, in: *An Invariant Approach to the Statistical Analysis of Shapes*, S. Lele and J. T. Richtsmeier, eds., Chapman and Hall/CRC Press, London, pp. 263–284.

Davison, A. C. and Hinkley, D. V., 1997, *Bootstrap Methods and their Applications*, Cambridge University Press, Cambridge.

Davisson, M., Schmidt, C., Reeves, N., Irving, E., Akeson, E., Harris, B. et al., 1993, Segmental trisomy as a mouse model for Down Syndrome, *Prog. Clin. Biol. Res.* 384:117–133.

Delabar, J.-M., Theophile, D., Rahmani, Z., Chettouh, Z., Blouin, J.-L., Prieut, M., Noel, B., and Sinet, P.-M., 1993, Molecular mapping of twenty-four features of Down syndrome on Chromosome 21, *Eur. J. Hum. Genet.* 1:114–124.

DeLeon, V. B., 2004, *Fluctuating Asymmetry in the Human Craniofacial Skeleton: Effects of Sexual Dimorphism, Stress, and Developmental Anomalies*, PhD Thesis, Center for Functional Anatomy & Evolution, Johns Hopkins University.

Efron, B. and Tibshirani, R., 1993, *An Introduction to the Bootstrap*. Chapman & Hall, New York.

Fuller, R. and Houle, D., 2002, Detecting genetic variation in devleopmental instability by artificial selection on fluctuating asymmetry, *J. Evol. Biol.* 15: 954–960.

Greber-Platzer, S., Schatzmann-Turhani, D., Wollenek, G., and Lubec, G., 1999, Evidence against the current hypothesis of "gene dosage effects" of trisomy 21: ets-2, encoded on chromosome 21 is not overexpressed in hearts of patients with Down syndrome, *Biochem. Biophys. Res. Commun.* 254:395–399.

Hall, B., 1965, Delayed ontogenesis in human trisomy syndromes, *Hereditas* 52:334–344.

Hall, P. and Martin, M., 1988, On the bootstrap and two-sample problems, *Austral. J. Stat.* 30A:179–192.

Hallgrímmson, B. and Hall, B., 2002, Modularity within and among limbs: Implications for evolutionary divergence in fore- and hind limb morphology in primates, *Am. J. Phys. Anthropol. Suppl.* 34:81 (abstract).

Hattori, M., Fujiyama, A., Taylor, T. D., Watanabe, H., Yada, T., Park, H. S. et al., 2000, The DNA sequence of human chromosome 21, *Nature* 405:311–319.

Hill, C., Reeves, R. H., Epstein, C. J., Valeri, C. J., Lindsay, E., Baxter, L. L. Cole, T. M., Richtsmeier, JT, 2003, Developmental instability and skeletal phenotypes in Down syndrome, *Am. J. Phys. Anthropol. Suppl.* 36:114 (abstract).

Kirschner, M. and Gerhart, J., 1998, Evolvability, *Proc. Natl. Acad. Sci. USA* 95:8420–8427.

Kisling, E., 1966, *Cranial Morphology in Down's Syndrome: A Comparative Roentgencephalometric Study in Adult Males*, Munksgaard, Copenhagen.

Klingenberg, C., 2003, A developmental perspective on developmental instability: Theory, models and mechanisms, in: *Developmental Instability: Causes and Consequences*, M. Polak, ed., Oxford University Press, New York, pp. 427–442.

Klingenberg, C. and McIntyre, G., 1998, Geometric morphometrics of developmental instability: Analyzing patterns of fluctuating asymmetry with Procrustes methods, *Evolution* 52:1363–1375.

Klingenberg, C. P., Barluenga, M., and Meyer, A., 2002, Shape analysis of symmetric structures: Quantifying variation among individuals and asymmetry, *Evolution* 56:1909–1920.

Kohn, L. and Cheverud, J., 1992, Calibration, validation, and evaluation of scanning systems: Anthropmetric imaging system repeatability, in: *Electronic Imaging of the Human Body Workshop*, CSERIAC, Dayton, OH.

Korenberg, R., 1991, Down syndrome phenotypic mapping. Progress in clinical Biology, *Research* 373:43–53.

Korenberg, J. R., Kawashima, H., Pulst, S. M., Ikeuchi, T., Ogasawara, N., Yamamoto, K. et al., 1990, Molecular definition of a region of chromosome 21 that causes features of the Down syndrome phenotype, *Am. J. Hum. Genet.* 47:236–246.

Korenberg, J., Chen, X., Schipper, R., Sun, Z., Gonsky, R., Gerwehr, S. et al., 1994, Down syndrome phenotypes: The consequences of chromosomal imbalance, *Proc. Natl. Acad. Sci. USA* 91:4997–5001.

Lande, R., 1977, On comparing coefficients of variation, *Syst. Zool.* 26:214–217.

Lele, S., 1991, Some comments on coordinate free and scale invariant methods in morphometrics, *Am. J. Phys. Anthropol.* 85:407–418.

Lele, S., 1993, Euclidean distance matrix analysis (EDMA) of landmark data: Estimation of mean form and mean form difference, *Math. Geol.* 25:573–602.

Lele, S. and McCulloch, C., 2002, Invariance and morphometrics, *J. Am. Stat. Assoc.* 971:796–806.

Lele, S. and Richtsmeier, J., 1990, Statistical models in morphometrics: Are they realistic? *Syst. Zool.* 39:60–69.

Lele, S. and Richtsmeier, J. T., 1992, On comparing biological shapes: Detection of influential landmarks, *Am. J. Phys. Anthropol.* 87:49–65.

Lele, S. and Richtsmeier, J., 2001, *An Invariant Approach to the Statistical Analysis of Shapes*, Chapman and Hall/CRC Press, London.

Levinson, A., Friedman, A., and Stamps, F., 1955, Variability of mongolism, *Pediatrics* 16:43.

Marcus, L., Corti, M., Loy, A., Naylor, G. J. P., and Slice, D. E., 1996, *Advances in Morphometrics*, Plenum, New York.

Mardia, K., Bookstein, F., and Moreton, I., 2000, Statistical assessment of bilateral symmetry of shapes, *Biometrika* 87:285–300.

McAdams, H. H. and Arkin, A., 1997, Stochastic mechanisms in gene expression, *Proc. Natl. Acad. Sci. USA* 94:814–819.

Møller, A. and Swaddle, J., 1997, *Asymmetry, Developmental Stability, and Evolution*, Oxford University Press, Oxford.

Neville, A., 1976, *Animal Asymmetry*, Edward Arnold, London.

O'Grady, K. F. and Antonyshyn, O. M., 1999, Facial asymmetry: Three-dimensional analysis using laser scanning, *Plast. Reconstr. Surg.* 104:928–940.

Palmer, A., 1994, Fluctuating asymmetry: A primer, in: *Developmental Instability: Its Origins and Implications*, T. Markow, ed., The Netherlands, Kluwer, Dordrecht, pp. 335–364.

Palmer, A. R., 1996, From symmetry to asymmetry: Phylogenetic patterns of asymmetry variation in animals and their evolutionary significance, *Proc. Natl. Acad. Sci. USA* 93:14279–14286.

Palmer, A. and Strobeck, C., 1986, Fluctuating asymmetry: Measurement, analysis, patterns, *Ann. Rev. Ecol. Syst.* 17:391–421.

Palmer, A. and Strobeck, C., 1992, Fluctuating asymmetry as a measure of developmental stability: Implications of non-normal distributions and power of statistical tests, *Acta Zool. Fenn* 191:57–72.

Polak, M., 2003, *Developmental Instability: Causes and Consequences*, Oxford University Press, Oxford.

Pritchard, M. A. and Kola, I., 1999, The "gene dosage effect" hypothesis versus the "amplified developmental instability" hypothesis in Down syndrome, *J. Neural Transm. Suppl.* 57:293–303.

Reeves, R., Irving, N., Moran, T., Wohn, A., Kitt, C., Sisodia, S. et al., 1995, A mouse model for Down syndrome exhibits learning and behavior deficits, *Nat. Genet.* 11:177–184.

Reeves, R. H., Baxter, L. L., and Richtsmeier, J. T., 2001, Too much of a good thing: Mechanisms of gene action in Down syndrome, *Trends Genet.* 17:83–88.

Richtsmeier, J., Cheverud, J., and Lele, S., 1992, Advances in anthropological morphometrics, *Ann. Rev. Anthropol.* 21:231–253.

Richtsmeier, J. T., Paik, C. H., Elfert, P. C., Cole, T. M., and Dahlman, H. R., 1995, Precision, repeatability, and validation of the localization of cranial landmarks using computed tomography scans, *Cleft Palate Craniofac. J.* 32:217–227.

Richtsmeier, J. T., Baxter, L. L., and Reeves, R. H., 2000, Parallels of craniofacial maldevelopment in Down syndrome and Ts65Dn mice, *Dev. Dyn.* 217:137–145.

Richtsmeier, J., DeLeon, V., and Lele, S., 2002a, The promise of geometric morphometrics, *Yearb. Phys. Anthropol.* 45:63–91.

Richtsmeier, J. T., Zumwalt, A., Carlson, E. J., Epstein, C. J., and Reeves, R. H., 2002b, Craniofacial phenotypes in segmentally trisomic mouse models for Down syndrome, *Am. J. Med. Genet.* 107:317–324.

Richtsmeier, J., Leszl, J., Hill, C., Aldridge, K., Aquino, V. et al., 2002c, Development of skull dysmorphology in Ts65Dn segmentally trisomic mice, *Am. J. Hum. Genet. Suppl.* 72:280 (abstract).

Richtsmeier, J. T., T. M. Cole III, Leszl, J. M., Hill, C. A., Budd, J. L., and Reeves, R. H., 2003, Developmental instability of the skull in aneuploidy, *European Society for Evolutionary Biology, 9th Congress*, Leeds, August (abstract).

Roche, A., 1964, Skeletal maturation rates in mongolism, *Am. J. Roentgenol.* 91:979–987.

Roche, A., 1965, The stature of mongols, *J. Ment. Defic. Res.* 9:131–145.

Rohlf, F. J. and Slice, D. E., 1990, Extensions of the procrustes method for the optimal superimposition of landmarks, *Syst. Zool.* 39:40–59.

Sago, H., Carlson, E., Smith, D., Kilbridge, J., Rubin, E., Mobley, W. et al., 1998, Ts1Cje, a partial trisomy 16 mouse model for Down syndrome, exhibits learning and behavioral abnormalities, *Proc. Natl. Acad. Sci. USA* 95:6256–6261.

Sago, H., Carlson, E., Smith, D. J., Rubin, E. M., Crnic, L. S., Huang, T. T. et al., 2000, Genetic dissection of region associated with behavioral abnormalities in mouse models for Down syndrome, *Pediatr. Res.* 48:606–613.

Saran, N. G., Pletcher, M. T., Natale, J. E., Cheng, Y., and Reeves, R. H., 2003, Global disruption of the cerebellar transcriptome in a Down syndrome mouse model, *Hum. Mol. Genet.* 12(16):2013–2019.

Shapiro, B., 1970, Prenatal dental anomalies in mongolism: Comments on the basis and implications of variability, *Ann. NY Acad. Sci.* 171:562–577.

Shapiro, B., 1975, Amplified developmental instability in Down syndrome, *Ann. Hum. Genet.* 38:429–437.

Shapiro, B., 1983, Down syndrome—a disruption of homeostasis, *Am. J. Med. Genet.* 14:241–269.

Shapiro, B. L., 1999, The Down syndrome critical region, *J. Neural. Transm. Suppl.* 57:41–60.

Shapiro, B. L., 2001, Developmental instability of the cerebellum and its relevance to Down syndrome, *J. Neural Transm. Suppl.* 61 11–34.

Siegel, A. and Benson, R., 1982, A robust comparison of biological shapes, *Biometrics* 38:341–350.

Smith, D., Crespi, B., and Bookstein, F., 1997, Fluctuating asymmetry in the honey bee, *Apis mellifera*: Effects of ploidy and hybridzation, *J. Evol. Biol.* 10:551–574.

Van Valen, L., 1962, A study of fluctuating asymmetry, *Evolution* 16:125–142.

Wagner, G., 1995, Adaptation and the modular design of organisms, in: *Advances in Artificial Life*, A. Moran, J. Merelo, and P. Chacon, eds., Springer-Verlag, Berlin, pp. 317–328.

Walker, J., 2001, Ability of geometric morphometric methods to estimate a known covariance matrix, *Syst. Biol.* 49:686–696.

Zakharov, V., 1992, Population phenogenetics: Analysis of developmental stability in natural populations, *Acta Zool. Fenn* 191:7–30.